

Atomic Decoration of a Random-Cluster Model for Icosahedral-Phase AlMnSi

J. L. Robertson^(a) and S. C. Moss

Department of Physics, University of Houston, Houston, Texas 77204-5504

(Received 26 October 1990)

Preliminary results on the atomic decoration of a random-cluster model for icosahedral-phase alloys are presented. The calculated neutron and x-ray intensities compare quite favorably with experimental intensity data on *i*-AlMnSi. The origin of the peak at $Q = 1.62 \text{ \AA}^{-1}$, associated with the prepeak found in "amorphous" AlMnSi, as well as the ubiquitous "diffuse" scattering, seen experimentally under the groups of strong peaks in all icosahedral-phase alloys, are revealed selectively in the calculated partial intensities for Al-Al, Al-Mn, and Mn-Mn correlations.

PACS numbers: 61.42.+h, 61.50.Em, 61.55.Hg

We have recently reported on a random-cluster model (RCM) for icosahedral-phase (*i*-phase) alloys constructed by randomly packing icosahedral clusters with physically motivated constraints on the allowed local cluster configurations.¹ This model is a natural extension of earlier work by Shechtman and Blech² and Stephens and Goldman,³ and is complementary to the recent treatment by Elser.⁴ These models are thought to be entropically^{4,5} stabilized, as is the analogous random-tiling model,^{5,6} by the large number of nearly equivalent cluster configurations. Our model was shown to possess long-range translational order comparable to, or greater than, that found in simple *i*-phase alloys such as *i*-AlMnSi and *i*-AlLiCu, and the peak shapes and positions were in good agreement with experiment. In this Letter we present preliminary results on the atomic decoration of our model and show that the calculated x-ray and neutron powder diffraction patterns compare quite favorably with experimental intensities⁷ on *i*-AlMnSi.⁸ Taken together, our results would appear to support an approach to the *i*-phase alloys in which a physically sensible structure is grown and its atomic decoration then explored.

By "physically sensible" we mean that the icosahedral-phase AlMnSi has a closely related crystalline phase,⁹ α -AlMnSi, which is essentially a bcc packing of 54-atom icosahedral clusters.¹⁰ In the α phase the clusters are attached face to face along the body diagonals of the cubic lattice. Our modeling of *i*-AlMnSi packs the same icosahedral atomic clusters found (slightly distorted) in the α phase, but connects their faces at random, ignoring the bcc lattice as in Refs. 2, 3, and 4. In addition, we have imposed constraints on the local cluster configurations by introducing three adjustable parameters as described in detail in Ref. 1. The particular model discussed in this Letter was constrained to grow in concentric spherical shells of thickness $\Delta S = 2.2 \text{ \AA}$ (0.2 of the cluster separation distance), and a shell was considered full when the probability of finding a usable face fell below a cutoff probability $P = \frac{1}{500}$. The size of the explored local environment of a cluster was $L = 17.5 \text{ \AA}$ ($L = 1.6$ model units in Ref. 1), i.e., only a discrete set of

neighbor distances less than L were permitted for each cluster. It should also be noted that in the α phase 22% of the atoms, all Al(Si), are not part of a 54-atom cluster and fill the space between the clusters. These atoms, often referred to as "glue," are highly correlated with the clusters and can be associated with a third (incomplete) icosahedral shell where each atom belongs to more than one cluster.¹¹

Although our most ordered model, $L = 21.9 \text{ \AA}$ (see Ref. 1), has a cluster density that is $\sim 90\%$ of the α -phase density, the diffraction peaks are narrower than those found in the data despite the limited model size, $\sim 550 \text{ \AA}$ in diameter. This indicates that the translational correlation range is greater than that of the real *i*-AlMnSi material. Hence we have chosen the $L = 17.5\text{-\AA}$ model (whose phason strain is slightly greater) for decoration, which has a cluster density $\sim 85\%$ of that of the α phase. The calculated diffraction intensities discussed here then represent only 66% of the total number of atoms (both density and stoichiometry are nearly the same in the *i* and α phases¹²) because we have not yet included the glue atoms in the decoration; in other words, at this point we are only considering the scattering of the 54-atom cluster ensemble. In this sense the results presented here are preliminary and work is currently in progress, based on Henley's canonical tilings,¹³ to account for all the atoms. Nonetheless, as we shall see, one can learn a great deal from this preliminary solution to the full structure.

The calculated powder diffraction pattern for the undecorated model is presented in Fig. 1 for a 330- \AA assembly of 15 803 icosahedral clusters. In Fig. 2 we show the partial neutron intensities, partial x-ray intensities, and the combined total neutron and x-ray intensities together with experimental neutron and x-ray data. We have calculated powder patterns because we are interested in the total scattered intensity, including background. This continuous powder pattern thereby includes both structural disorder as well as the envelope of all the weak peaks (large Q^\perp).¹⁴ The powder structure factor $S(Q)$ for the undecorated model is calculated by assigning a

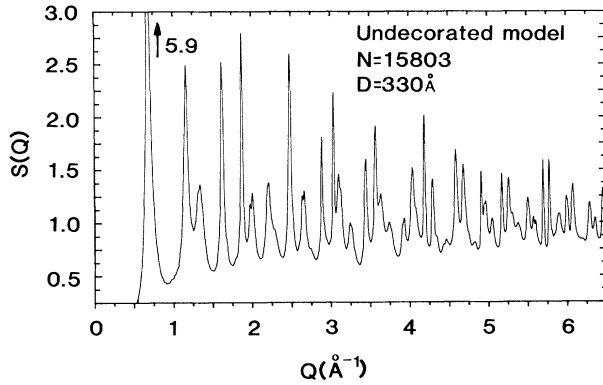


FIG. 1. The calculated $S(Q)$ for the undecorated model. The peak shapes and positions are in good agreement with the neutron [Fig. 2(e)] and x-ray [Fig. 2(j)] intensity data on i -AlMnSi.

scattering power of 1.0 to each cluster center and Fourier transforming $G(r)$, the deviation from the average number density, which has been corrected for the finite model size.¹⁵ The $S(Q)$ is given by

$$S(Q) - 1 = \int_0^\infty G(r) \frac{\sin(Qr)}{Qr} dr, \quad G(r) = 4\pi r^2 [\rho(r) - \rho_0],$$

where $Q = 4\pi \sin(\theta)/\lambda$, $\rho(r)$ is the density as a function of r averaged over every cluster as the origin, and ρ_0 is the (r -dependent¹⁵) average density. We use a small sphere (~ 330 Å across) taken from the larger model to bring the amount of computer time used on the decorated model to within a reasonable amount, ~ 100 h on a Cray 2 computer. Unfortunately there are no shortcuts if *all* of the intensity is to be included.

In order to calculate the diffracted intensity from the decorated model, we first calculate the partial pair-correlation functions¹⁵ $G^{\alpha\beta}(r)$. The total neutron intensity is given by

$$I(Q) = \sum_{i=\alpha,\beta} x_i b_i^2 + \sum_{i=\alpha,\beta} \sum_{j=\alpha,\beta} \frac{x_i b_i b_j}{N_i} \int_0^\infty G^{i-j}(r) \frac{\sin(Qr)}{Qr} dr,$$

where x_i is the concentration of the i th atomic species, N_i is the number of atoms of the i th type in the model, and b_i is the neutron scattering length in 10^{-12} cm. The partial scattering intensities $I^{\alpha\beta}(Q)$ are then given by

$$\begin{aligned} I^{\text{Mn-Mn}}(Q) &= x_{\text{Mn}} b_{\text{Mn}}^2 \\ &\quad + \frac{x_{\text{Mn}} b_{\text{Mn}}^2}{N_{\text{Mn}}} \int_0^\infty G^{\text{Mn-Mn}}(r) \frac{\sin(Qr)}{Qr} dr, \\ I^{\text{Al-Al}}(Q) &= x_{\text{Al}} b_{\text{Al}}^2 + \frac{x_{\text{Al}} b_{\text{Al}}^2}{N_{\text{Al}}} \int_0^\infty G^{\text{Al-Al}}(r) \frac{\sin(Qr)}{Qr} dr, \\ I^{\text{Mn-Al}}(Q) &= \frac{2x_{\text{Mn}} b_{\text{Mn}} b_{\text{Al}}}{N_{\text{Mn}}} \int_0^\infty G^{\text{Mn-Al}}(r) \frac{\sin(Qr)}{Qr} dr. \end{aligned}$$

The x-ray intensities have exactly the same form with b replaced by $f(Q)$, the x-ray mean atomic scattering factor, which, unlike b , is Q dependent. A weighted average was used for b_{Al} and $f_{\text{Al}}(Q)$ to account for the Si. Because of the preliminary nature of the calculation, no Debye-Waller factors were included.

The undecorated $S(Q)$, Fig. 1, has peak shapes and peak positions that are in good agreement with the neutron [Fig. 2(e)] and x-ray [Fig. 2(j)] intensity data; every peak in each experimental powder pattern has a corresponding peak in the undecorated $S(Q)$. Note that there are corresponding peaks that are strong (weak) in the x-ray data and weak (strong) in the neutron data (for example, the peaks at $Q \approx 2.89, 3.04, 5.72$, and 5.80 Å⁻¹). These differences are due to the difference in scattering contrast between Mn and Al for neutrons ($b_{\text{Mn}} = -0.38 \times 10^{-12}$ cm and $b_{\text{Al}} = 0.36 \times 10^{-12}$ cm) and x rays (12-electron difference) which means that the neutron data emphasize the “difference lattice” while the x-ray pattern emphasizes the “average lattice.”

The partial intensities are quite instructive in determining which atomic correlations give rise to various features in the experimental diffraction patterns. For instance, consider the two peaks at $Q \approx 5.72$ and 5.80 Å⁻¹ which have relatively small values of Q^\perp but are absent in the neutron data. The Mn-Mn and Al-Al partial intensities both have a positive contribution for these peaks while the Mn-Al partial intensity is negative and nearly cancels the other contributions. For x rays all three partial intensities give a positive contribution at these positions. Of even greater interest is the peak at $Q = 1.62$ Å⁻¹ which is almost entirely due to Mn-Mn correlations. In the “amorphous” diffraction pattern of AlMnSi of the same composition there is a prepeak at this position.¹⁶ Such a prepeak is usually associated with correlations in the minority atomic species¹⁷ and in this case has been identified with the Mn-Mn distance of ~ 4.5 Å.¹⁶ The partial intensities shown here demonstrate that this remains the case in the quasicrystal which is of particular interest because the broadened quasicrystal pattern agrees so well with the amorphous pattern.¹⁶

We also note the “diffuse” intensity found under the groups of strong peaks near $Q \approx 2.7$ and 5.0 Å⁻¹ with weaker diffuse scattering at $Q \approx 3.5$ and 5.8 Å⁻¹, all of which seems to resemble closely the main features in the amorphous diffraction pattern.^{16,18} Such diffuse scattering, which is common to all of the i -phase alloys studied thus far, including those thought to be free of phason strain (e.g., i -AlFeCu or i -AlRuCu), is clearly visible in the total-intensity plots although it does not seem to be in the undecorated $S(Q)$. By examining the partial intensities we see that the diffuse scattering appears predominantly in the Al-Al correlations. It is interesting that this feature is reproduced without either the glue atoms or any substitutional disorder within the atomic clusters. At least for i -AlMnSi, this must result from weak peaks with large Q^\perp that are part of the back-

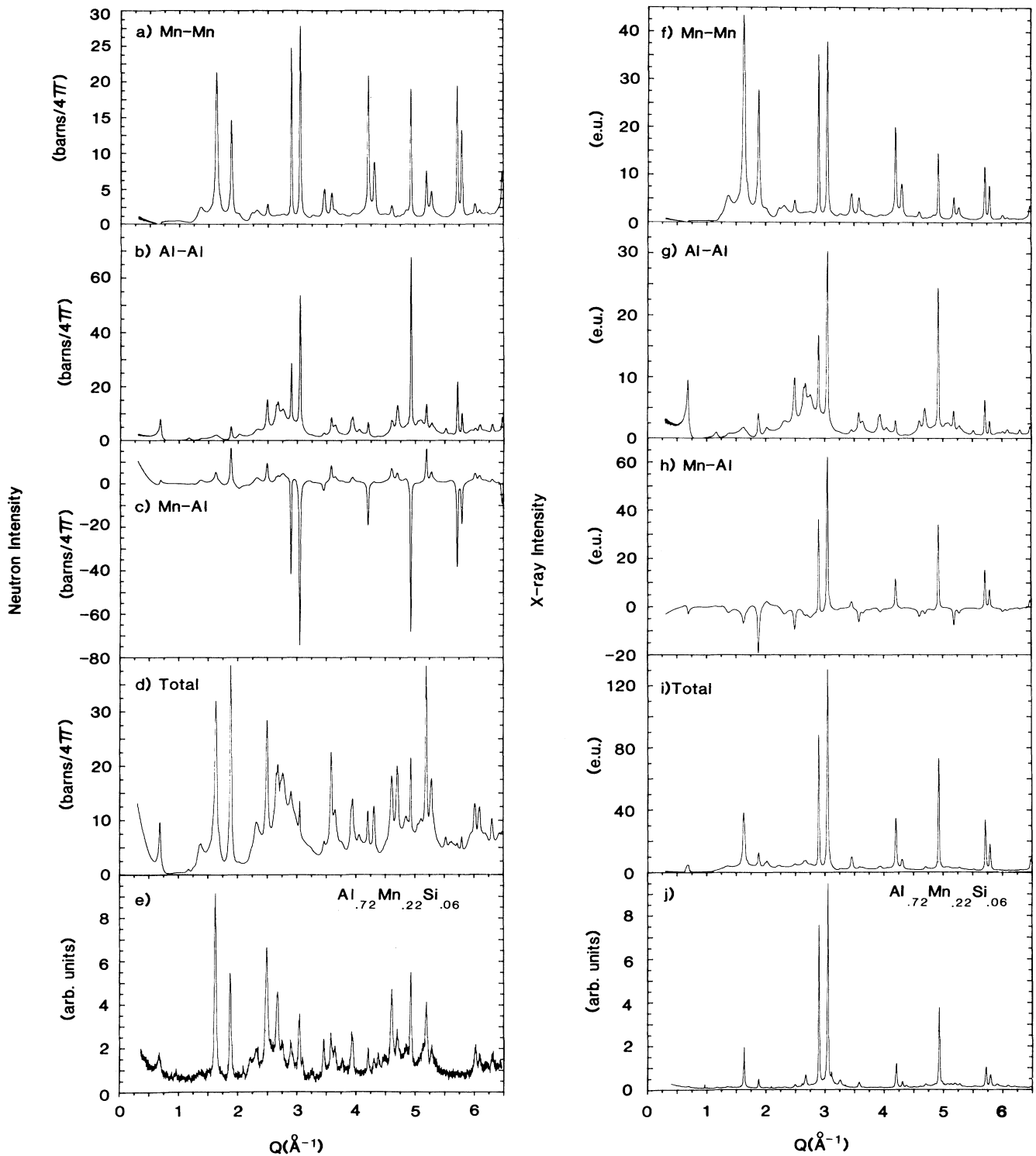


FIG. 2. Partial neutron scattering intensity, in barns/steradian, calculated for (a) Mn-Mn, (b) Al-Al, and (c) Mn-Al correlations; (d) total neutron intensity and (e) experimental neutron intensity data on *i*-AlMnSi. Partial calculated x-ray intensity, in electron units (e.u.), for (f) Mn-Mn, (g) Al-Al, and (h) Mn-Al correlations; (i) total x-ray intensity and (j) experimental x-ray intensity data on the same *i*-AlMnSi material as in (e).

ground in the undecorated $S(Q)$ (Ref. 14) but are more heavily weighted in the Al-Al partial intensity. This has been confirmed by a calculation of the structure factor for a single 54-atom icosahedron in which strong broad peaks appear in the Al-Al partial intensity at ~ 2.8 and $\sim 5.0 \text{ \AA}^{-1}$ which are not in the Mn-Al or Mn-Mn functions. At these $|Q^{\parallel}|$ ($\equiv Q$) positions, however, these strong Al-Al contributions appear about symmetry axes where the Bragg peaks due to the model are weak (i.e., large $|Q^{\perp}|$). To be specific, the prominent experimental peaks at $|Q^{\parallel}|=2.89$ and 3.04 \AA^{-1} are on the fivefold and twofold axes, respectively, while the strong Al-Al contribution at $|Q^{\parallel}| \approx 3.0 \text{ \AA}^{-1}$ is along the threefold axis of the 54-atom icosahedron.

The agreement with the calculated total intensities cannot be perfect, of course, because 33% of the atoms are missing. In addition, the x-ray patterns are in better agreement than are the neutron patterns because neutrons will be more sensitive to the decoration in the glue than x rays. There are also other, more curious, differences, such as the peak at $Q \sim 3.45 \text{ \AA}^{-1}$ which is much weaker in the calculated neutron pattern than in the data but is much stronger in the calculated x-ray pattern. Our partial intensities, nonetheless, compare well with the neutron study of contrast variation in Al-transition-metal alloys by Janot *et al.*¹⁹

An important theme in structural studies of *i*-phase alloys has been the 6D Patterson analysis²⁰ from which an average 6D lattice can be determined and the real 3D structure inferred. Criticism by its practitioners²¹ of the sole use of this procedure has, however, recently appeared. We thus offer the present results as a preliminary attempt to provide an alternative in which the *i*-phase alloy may be viewed as a decorated RCM with quenched-in phason strain.¹

The authors wish to thank B. Mozer for kindly supplying the neutron data. We also gratefully acknowledge the support of the Department of Energy, Division of Basic Energy Science, Grant No. DE-FG05-87ER45325, and the use of the computer resources of the National Energy Research Supercomputer Center at the LLNL.

^(a)Current address: National Institute of Standards and Technology, Reactor Building, Gaithersburg, MD 20899.

¹J. L. Robertson and S. C. Moss, *Z. Phys. B Condens. Matter* (to be published).

²D. Schechtman and I. A. Blech, *Metall. Trans. A* **16**, 1005 (1985).

³P. W. Stephens and A. I. Goldman, *Phys. Rev. Lett.* **56**, 2331 (1986); P. W. Stephens, in *Aperiodicity and Order 3: Extended Icosahedral Structures*, edited by M. V. Jarić and D. Gratias (Academic, San Diego, 1989), p. 37.

⁴V. Elser, in *Aperiodicity and Order 3: Extended Icosahedral Structures* (Ref. 3), p. 105.

⁵K. J. Strandburg *et al.*, *Phys. Rev. Lett.* **63**, 314 (1989); M. Widom *et al.*, *Phys. Rev. Lett.* **63**, 310 (1989).

⁶L.-H. Tang, *Phys. Rev. Lett.* **64**, 2390 (1990); L.-H. Tang and M. V. Jarić, *Phys. Rev. B* **41**, 4524 (1990).

⁷The x-ray data were taken on beam line X-14 of the Oak Ridge National Laboratory at the National Synchrotron Light Source. Neutron data supplied by B. Mozer, National Institute of Standards and Technology.

⁸Sample prepared by J. Bigot and co-workers at Centre d'Etudes de Chimie Métallurgique, Vitry-sur-Seine, France.

⁹M. Audier *et al.*, *Philos. Mag.* **B 54**, 105 (1986); C. L. Henley and V. Elser, *Philos. Mag.* **53**, L59 (1988).

¹⁰M. Cooper and K. Robinson, *Acta Crystallogr.* **20**, 614 (1966); C. Rømming and J. E. Tibballs (to be published).

¹¹H. A. Fowler *et al.*, *Phys. Rev. B* **37**, 3906 (1988).

¹²Ch. Janot *et al.*, *Philos. Mag.* **B 58**, 59 (1988); R. J. Schaefer and L. A. Bendersky, in *Aperiodicity and Order 1: Introduction to Quasicrystals*, edited by M. V. Jarić (Academic, San Diego, 1988), p. 111.

¹³C. L. Henley, *Phys. Rev. B* **43**, 993 (1991).

¹⁴Y. Ma *et al.*, *Phys. Rev. B* **40**, 8053 (1989); X.-O. Li *et al.*, *Phys. Rev. B* (to be published).

¹⁵J. L. Robertson and S. C. Moss, *J. Non-Cryst. Solids* **106**, 330 (1988).

¹⁶J. L. Robertson *et al.*, *Phys. Rev. Lett.* **60**, 2062 (1988).

¹⁷S. C. Moss and D. L. Price, in *Physics of Disordered Materials*, edited by D. Adler, H. Fritzsche, and S. R. Ovshinsky (Plenum, New York, 1985).

¹⁸J. M. Dubois *et al.*, *J. Non-Cryst. Solids* **93**, 179 (1987).

¹⁹Ch. Janot *et al.*, *Europhys. Lett.* **3**, 995 (1987).

²⁰J. W. Cahn *et al.*, *J. Phys. (Paris)* **49**, 1225 (1988); S.-Y. Qiu and M. V. Jarić, in *Quasicrystals*, edited by M. V. Jarić and S. Lundqvist (World Scientific, Singapore, 1990), p. 19.

²¹M. De Boissieu *et al.* (to be published).